Light-Enhanced Micropyramidal Sensors for Interleukin-6 Impedance Detection

Foram Madiyar*
Department of Physical Science,
1, Aerospace Blvd,
Daytona Beach, Florida, 32114
madiyarf@erau.edu
Corresponding author

Kaitlyn Nielsen
Department of Physical Science,
1, Aerospace Blvd,
Daytona Beach, Florida, 32114
nielsek4@my.erau.edu

Sahil Ghate
Department of Aerospace Engineering,
1, Aerospace Blvd,
Daytona Beach, Florida, 32114
ghates@my.erau.edu

Rishikesh Srinivasaraghavan Govindarajan
Department of Aerospace Engineering,
1, Aerospace Blvd,
Daytona Beach, Florida, 32114
srinivr1@my.erau.edu

Daewon Kim
Department of Aerospace Engineering,
1, Aerospace Blvd,
Daytona Beach, Florida 32114
kimd3c@erau.edu

***Abstract*—The inflammation marker Interleukin 6 (IL-6) typically remains below 5 pg/mL in the serum of healthy individuals but can increase tenfold during inflammation in chronic conditions like COVID-19 and rheumatoid arthritis, as well as acute conditions like sepsis. This study is focused on the rapid detection of IL-6 to monitor both chronic and acute diseases. The novel sensor, designed with gold-coated micropyramids on the electrodes, was fabricated using the two-photon polymerization method, enabling low-volume sensing capabilities (2-3 µL). The micropyramids were surface functionalized with interleukin-6 antibodies towards developing an affinity biosensor specific to the physiological relevant range of IL-6 of 5.1 and 18.8 pg/mL in mild inflammation. Sensing was achieved by measuring impedance changes associated with IL-6 binding to the antibodies on the micropyramids interfaced using electrochemical impedance spectroscopy. It was observed that the signals from the lowest detection concentration was enhanced by 3 times at 1500 hz when the 532 nm green laser was incident on the micropyramids. This innovative approach can be expanded to the detection of cytokines not only in serum but also in respiratory samples. As a result, it opens up new avenues for monitoring local inflammation within the lungs and assessing systemic inflammation levels throughout the body.**

TABLE OF CONTENTS

1. INTRODUCTION

Traditional diagnostic methods for biomarkers and biochemical parameters often involve specialized labs and expert personnel, leading to extended test times, high reagent consumption, and overall inefficiency. In contrast, point-of-care testing (POCT) technology has emerged as a game-changer in health monitoring and disease diagnostics by miniaturizing diagnostic tools. This innovation offers a range of advantages, including smaller sample sizes, reduced reagent use, user-friendly interfaces, compact designs, and rapid results. The continuous wave of innovation in sensors, bioelectronics, and wearables has paved the way for advanced integrated POCT systems, pushing the boundaries of personal healthcare and precision medicine [1, 2]. However, the accurate measurement of biomarkers in biofluids like blood, urine, and saliva remains a challenge due to the presence of numerous molecules, ions, and proteins.

Dynamic monitoring of specific biomarkers is crucial for diagnosing various conditions, especially when the body is subjected to external stresses such as extended periods of isolation, radiation exposure, space travel, and overall health maintenance [3, 4]. Early detection, particularly in the case of cytokine storms caused by a surge in pro-inflammatory cytokines, is paramount for preventing disease progression and ensuring better outcomes [5-8]. Life-threatening complications such as Cytokine release syndrome (CRS) and sepsis often result from infections and other triggers. Elevated levels of Interleukin-6 (IL-6) frequently serve as indicators for these complications. Swift detection is crucial

979-8-3503-0462-6/24/$31.00 ©2024 IEEE

for early intervention, as it can reduce ICU admissions and intensive immunosuppressive treatments [3, 9-12].

However, traditional IL-6 detection methods, such as the enzyme-linked immunosorbent assay (ELISA) [13], offer precision but can take up to two days, hindering rapid point-of-care monitoring. While faster ELISA kits and ELISpot methods exist, they exhibit varying detection ranges and sensitivities [14]. The lateral flow assay (LFA) provides a quicker solution for point-of-care needs, especially those utilizing immunofluorescent techniques and gold nanoparticles [15]. Yet, challenges related to sample volume and viscosity can limit their applicability. Advanced methods like flow cytometry and Luminex bead-based assays offer sensitive, multiplexed detection but come with high costs, specialized handling requirements, and challenges related to lab standardization, cytokine stability, and sample handling [16, 17].

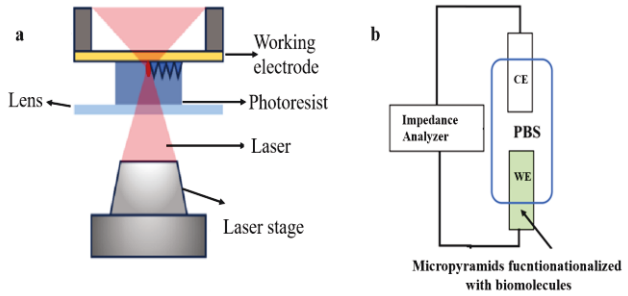

Figure 1. (a) Schematic image of the two-photon polymerization. The two beams focus on the photoresist to fabricate the micropyramids on the surface of the electrode of 4.0 μm in base length and height and (b) The schematic image of the experimental set up, where WE: is working electrode on which micropyramids are fabricated. CE: counter electrode

Researchers have intensified their efforts to advance cytokine detection tools, aiming to improve sensitivity and enable multiplexed detection. Innovations include biosensing platforms utilizing fluorescence or electrochemical signals, deployable devices for tracking spatially localized cytokines, and impedance aptasensors designed for IL-6 detection. The CRISPR/Cas biosensing system has demonstrated remarkable sensitivity in cytokine detection, achieving low limits of detection for human IL-6[18]. Multiplex detection of cytokines, such as IL-6, IL-1β, and TNF-α, has been achieved through a sandwich immunosensor, offering faster results akin to ELISA [16]. Additionally, spatial coding methods, surface-enhanced Raman scattering (SERS) [19], and microfluidic technologies have shown impressive sensitivity and potential for multi-cytokine detection [20], although they may still face challenges with cross-reactivity. Despite these advances in cytokine detection, many methods require multiple manual steps, resulting in workload challenges and potential inconsistencies. Therefore, there is a pressing need for point-of-care platforms that simplify cytokine detection, allowing real-time monitoring without extensive equipment or preparation.

Recent advancements in additive manufacturing (AM) have paved the way for the fabrication of high-resolution, bio-inspired structures. Among the various 3D printing methods such as fused deposition modeling (FDM), selective laser melting (SLM), and digital light processing (DLP) are central to creating innovative surfaces, two-photon polymerization (2PP) stands out for its unparalleled spatial resolution, enabling the creation of features smaller than Abbe's diffraction limit through non-linear light-induced effects in the photosensitive material. Typically, the 2PP process utilizes pulsed lasers with repetition rates in the tens of MHz range and light sources in green, near infrared, or a combination of these wavelengths [21]. In 2PP 3D printing, solid structures are created within a liquid resin, voxel by voxel, by precisely scanning a femtosecond-pulsed laser beam as shown in figure 1a [22]. As 2PP systems become more widespread, there is a growing interest in comparing different 2PP systems and evaluating their dimensional accuracy [23].

This paper introduces a novel low volume sensing platform that builds an affinity-based detection mechanism for detecting Interleukin-6 antigens utilizing the micropyramid structures on the existing electrodes fabricated through the two-photon polymerization method with unparalleled precision and intricacy. These micropyramids not only provide a greater surface area, facilitating enhanced biomolecule attachment, but also exhibit an exceptional capability to amplify impedance signals in the presence of laser light. The microstructures increase the sensitivity of the sensor even further to detect Interleukin-6 across physiologically relevant concentrations while providing a location for cross-linker binding. This innovative combination of structure and detection methodology promises to open new avenues in various fields, including biotechnology and sensor development, by offering superior sensitivity and performance. The presented micropyramids functionalized biosensor demonstrates a limit of detection for Inelukin-6 of 0.1 pg/mL on both the lab potentiostats. This range sufficiently covers the physiological expressed range of interleukin-6 in human sweat reported between of 5.1 and 18.8 pg/mL in the serum in the inflammatory conditions.

2. Materials and Methods

Materials:
The biosensor platform was purchased from Dropsense, G-MEA222 with 10 μm distance between the electrodes. The cross-linker 3, 3'-dithiobis (sulfosuccinimidyl propionate), Superblock and phosphate buffered saline (PBS), I Interlukin-6 (Int-6) antibodies, and Interlukin-6 (Int-6) antigen were purchased from Sigma Aldrich (MA, USA). All reagents were used as provided and without any purification.

Methods:

The biosensor platform is constructed with gold electrodes featuring precisely crafted 4x4x4.5 µm pyramid structures, often referred to as micropyramids. These micropyramids are intricately printed onto the working electrode using a sophisticated two-photon lithographic method. The process of creating and preparing this biosensor platform involves several crucial steps to ensure its functionality and reliability. Initially, the platform is submerged in deionized (DI) water for a duration of 3 minutes, followed by a 3-minute immersion in 99.5% acetone and an 8-minute bath in 99.9+% isopropyl alcohol (IPA). These cleaning steps are conducted within a sonicator to effectively remove any

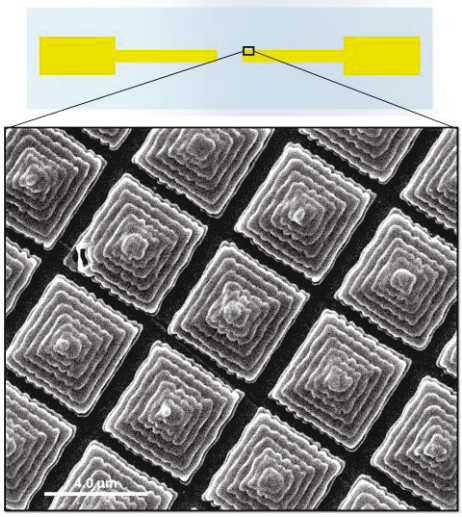

Figure 2. The image of the two-electrode system with the scanning electron microscope image of the micropyramids coated with golf and with scale bar of 4.0 µm

contaminants from the substrate. After the cleaning process, the substrate is meticulously dried using a stream of air to eliminate any residual moisture. Subsequently, the surface of the cleaned gold electrode undergoes activation through an oxygen plasma treatment, carried out using the Plasma Etch PE-50HF system from Plasma Etch, located in Caron City, USA. This treatment spans a duration of 40 seconds and is critical for enhancing the adhesion properties of the surface. The next step involves the deposition of a drop of IP-S photoresist, obtained from Nanoscribe in Eggenstein-Leopoldshafen, Germany, onto the center of the working electrode. This photoresist-coated electrode is then securely affixed to the substrate holder using polyimide tape. Once the 63x objective lens, meticulously cleaned with IPA, is installed in the 2PP printer, the substrate holder is carefully inserted into the printing area. The 63x objective lens is brought into close contact with the photoresist, initiating the polymerization process of the liquid photosensitive resin with the aid of a femtosecond laser beam. Following the completion of the base layers, the microstructures are meticulously crafted with a precise writing speed and 100% laser power setting, ensuring their accurate formation. Upon exiting the 2PP printer, the finished microstructures are transferred for development in propylene glycol methyl ether acetate (PGMEA), sourced from Merck KGaA in Darmstadt, Germany. This 20-minute development step serves to dissolve any excess uncured photosensitive resin, leaving behind only the desired microstructures. Subsequently, the structures are immersed in IPA for a 5-minute bath to eliminate any residual PGMEA residue. To enhance their functionality and conductivity, a thin layer of gold is uniformly coated onto the micropyramids. This gold coating process is accomplished using a 108 Manual sputter coater from Ted Pella, located in Redding, USA, and the coating duration typically lasts for 45 seconds.

In summary, the intricate process of constructing this biosensor platform involves a series of meticulously controlled steps, ranging from substrate cleaning and surface activation to precise polymerization and coating. Each step contributes to the platform's effectiveness in facilitating advanced biosensing applications.

Affinity assay functionalization protocols:

Following the fabrication of the sensor, a crucial series of steps were undertaken to prepare it for effective biomolecule immobilization. Initially, a 10 mM aqueous solution of 3,3'-dithiobis (sulfosuccinimidyl propionate) (DTSSP) crosslinker was delicately deposited onto the surface of the micropyramid situated on the working electrode. This deposition process was carried out meticulously, and the sensor was allowed to incubate in this DTSSP solution for a duration of 24 hours, maintaining a controlled room temperature environment. Subsequently, a precise washing procedure was performed using a 10-15 µL phosphate-buffered saline (PBS) solution to remove any unbound DTSSP crosslinkers from the sensor's surface. This step was essential to ensure that only the crosslinker molecules specifically bound to the sensor's micropyramids remained, creating a stable foundation for subsequent biomolecule attachment. The next critical phase involved the application of 2.0 µL of a solution containing Interleukin-6 (Int-6)

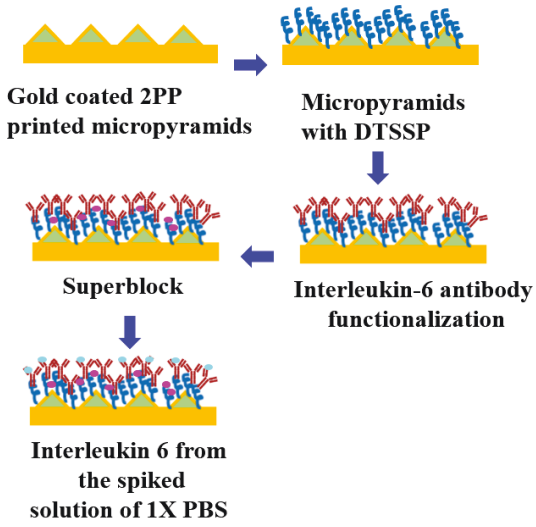

Figure 3. Schematic representation of the immunoassay building protocol for marker biosensing platform

antibodies at a concentration of 10 µg/mL. These antibodies were carefully added to the sensor's surface, where they formed specific bonds with the crosslinked DTSSP molecules. This step represents the immobilization of Int-6 antibodies onto the sensor, a pivotal process for its biosensing capabilities. To further refine the sensor's preparation, another round of washing was carried out using a 10-15 µL PBS solution. This wash was essential to remove any unbound antibodies that had not successfully adhered to the immobilized DTSSP crosslinkers, ensuring a high degree of specificity in antibody attachment. Finally, to prevent biofouling and maintain the sensor's functionality, a 2.0 µL solution of superblock was applied to the sensor's surface[24]. The superblock solution serves as a protective barrier, minimizing non-specific interactions and ensuring that the sensor remains free from unwanted contaminants during subsequent biomolecule detection processes.

Experimental Set up:
Following the surface functionalization process, various concentrations of the Int-6 antigen were prepared by spiking 1x PBS. These prepared samples were then subjected to characterization using electrochemical impedance spectroscopy (EIS) with the BODE-100 instrument, covering a frequency range from 1 Hz to 40 MHz. To establish a baseline, an initial measurement was performed using unspiked PBS. Subsequent measurements were taken as the concentrations of the Int-6 antigen were incrementally increased, starting from the lowest concentration and progressing to the highest. Each of these spiked samples was allowed to incubate for a consistent duration of 90 seconds before impedance measurements were recorded. It is important to note that during the functionalization steps, the volumes of reagents and samples used were carefully controlled, and they were maintained at or below 2.0 µL. This was done to account for the effective volume limitations of the sensor and to ensure accurate and reliable results. The sensors used in this experiment were configured in three distinct settings for comparative analysis. The first setting consisted of a control sensor featuring a flat gold electrode, devoid of micropyramids. In the second setting, micropyramids were present on the working electrode. Finally, the third setting involved micropyramids on the working electrode, with the additional application of a 532 nm wavelength light source (green laser: 532 nm) specifically focused on the microstructures. These different sensor configurations were designed to explore the impact of micropyramid structures and laser illumination on the EIS measurements, providing valuable insights into the detection capabilities of the system.

Infrared spectroscopy (ATR-FTIR):
Infrared spectra of the functionalization steps were carried out using the Agilent Cary 630 FTIR spectrometer with sampling stage with a 65° Germanium ATR crystal. ATR-FTIR specimens were prepared by drop casting the solutions on gold-coated glass slides with same surface functionalization protocol as mentioned previously. The contact area was about 1 cm^2. All spectra were recorded between 4000 and 400 cm^{-1} with a resolution of 4 cm^{-1} and 126 scans.

Scanning Electron Microscope Imaging:
Utilizing an FEI Quanta 650 scanning electron microscopy (SEM). The SEM imaging is performed at an acceleration voltage of 10 kV and in high vacuum mode to minimize the influence of atmospheric interference.

3. RESULTS

The figure 1a shows the 2PP polymerization set up for fabrication of the micropyramids, and figure 1 b shows the experimental set up with the micropyramids on the working electrode. The figure 2 shown the scanning electron microscope image of the micropyraminds with scale bar of 4.0 µm.The figure 3 illustrates the binding of the cross linker, Interleukin-6 antibody for the detection of the interleukin 6 antigen The FTIR spectrum is shown in figure 4a indicates the binding of the cross-linker on the sensor surface with NHS ester bond (peak at 1780 cm^{-1}) and free carboxylic acid peak (1740 cm^{-1}). The conjugation of both antibodies shows cleaving of C-O bond of NHS ester and the peak at 1780 cm^{-1} disappears, while enhanced aminolysis peak (at 1652 cm^{-1}) is observed confirming the binding of the antibody, as shown in figure 4b. Amine-reactive NHS ester reacts with primary amine of the antibody to form a stable amide bond. This phenomenon is seen by the disappearance of peak at 1743 cm^{-1} in the interleukin-6 spectra.

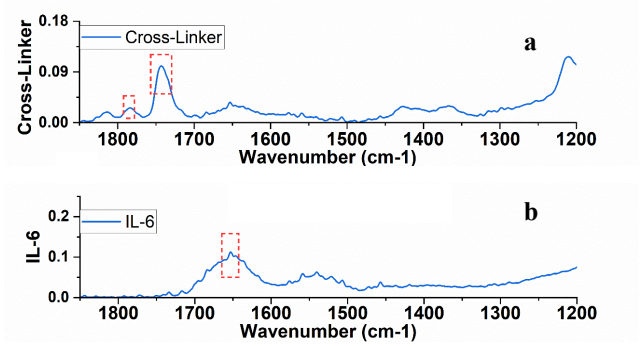

Figure 4. Infrared spectroscopy (ATR-FTIR) plots for the (a) crosslinked DTSSP and (b) after functionalization with interleukin-6

The interleukin-6 dose response is represented as Bode phase and magnitude plots in figure 5. |Z| reflects the total impedance of the system and can be used as a measure of both capacitive and resistance changes. In figure 5 represents as a percent change in |Z| impedance from the baseline measurement post-antibody functionalization at 1 kHz. There is a consistent increase in impedance as the dosage concentration of interleukin-6 increases. The percent change with respect to a post-functionalization baseline measurement was observed to be on the flat devoid of micropyramids is 2.9 % for 0.1pg/ml, 9.1 % for 1.0 pg/ml and 27.2 % for 10 pg/ml and with the micropyramids is 2.4 % for 0.1pg/ml, 5.8 % for 1.0 pg/ml and 5.8 % for 10 pg/ml. This is attributed to the micropyramid structure (4x4

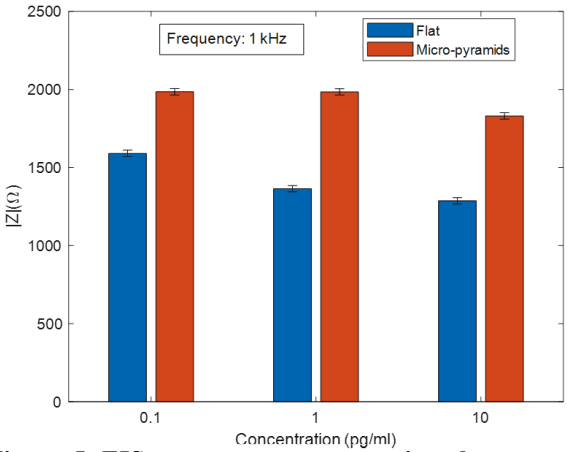

Figure 5. EIS measurement comparison between flat working electrode and micropyramids at varying concentration of Int-6: 0.1 pg/ml, 1.0 pg/ml, 10 pg/ml Int-6 concentration. The greatest change in impedance between flat working electrode and micropyramids was measured at 1 kHz

micrometers) fabricated by the 2PP method. This causes enhanced surface area for the attachments of interleukin 6 antibody. After theoretical calculations, the micropyramids increased with surface area by 6.0 times as compared to the flat surface. Additionally, higher surface concentration of interleukin-6 resulted in decrease in the real impedance value. This can be attributed to the accumulation of biomolecules within the EDL resulting in the changes in conductivity of solution. Additionally, in order to establish that the observed signal response was specific to the interleukin-6 binding events occurring on the flat electrodes and micropyrminds and not due to non-specific and physically absorbed mechanisms occurring on the glass

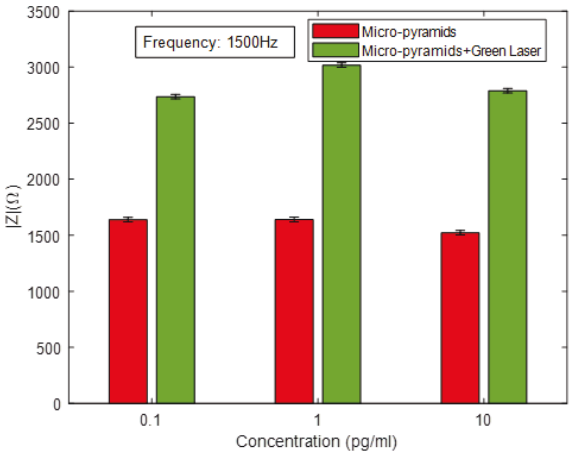

Figure 6. EIS measurement comparison between flat working electrode and micropyramids at varying concentration of Int-6: 0.1 pg/ml, 1.0 pg/ml, and 10 pg/ml Int-6 concentration. The greatest change in impedance between flat working electrode and micropyramids was measured at 1500Hz

substrate, a control study with the absence of DTSSP crosslinker was conducted. The protocol followed was identical to the one performed for the calibration dose response, but the DTSSP crosslinker used to bind the antibody to the gold surface was excluded. This left no place for the antibody to chemically bind upon the gold surface.

A similar investigation was carried out to measure Bode plots with different concentrations of 0.1 pg/ml, 1.0 pg/ml, and 10 pg/ml, both in the presence and absence of a green laser with a wavelength of 532nm, at frequencies of 1000 Hz and 1500 Hz, as shown in Figure 6. The percentage change relative to a post-functionalization baseline measurement at 1000 Hz was observed to be 1.6% for 0.1 pg/ml, 6% for 1.0 pg/ml, and 5.9% for 10 pg/ml when using micropyramids alone, and 45.6% for 0.1 pg/ml, 56.13% for 1.0 pg/ml, and 43.0% for 10 pg/ml when using micropyramids in conjunction with the green laser. This represents a 1.8 times enhancement in the presence of green light (532 nm). At a frequency of 1500 Hz, it was observed that the percentage increase with micropyramids combined with the green laser was 51.5% for 0.1 pg/ml, 63.8% for 1.0 pg/ml, and 48.6% for 10 pg/ml. This corresponds to a 3.0 times enhancement with light compared to the absence of green light (532 nm). This enhancement can be attributed to the ridges created during the two-photon polymerization (2PP) method. The gold-coated micropyramids' ridges interact with the green laser's electromagnetic field, leading to an enhancement in the impedance signal. Therefore, the choice of the detection frequency is crucial for achieving higher enhancement through exposure to laser light.higher enhancement through exposure to the laser light.

In a typical non-faradaic Nyquist plot, the absence of a redox label eliminates the parameters associated with electron transfer such as charge transfer resistance (Rct) and Warburg impedance by becoming infinite. This is represented by the large incomplete semicircle contributed due to the extremely slow electron transfer step, which is not followed by the typical diffusion tail. Therefore, in a non-faradaic electrochemical system, the imaginary part of impedance is inversely proportional to the electrical double layer capacitance. Furthermore, the binding interaction between the capture antibody and the target biomolecule at the electrode surface creates a charge perturbation. This phenomenon can be observed in where decrease in imaginary impedance is observed with increase in the concentration of interleukin-6. This can be leveraged to the capacitive change caused as a result of antibody-antigen binding complex within the EDL. The change in the dielectric permittivity causes a change in the double layer capacitance. Therefore, the decrease in impedance can be interpreted as a result of increase in interleukin-6 concentration [25].

The Nyquist plot in figure 7 shows how the EIS response changed with respect to increasing dose of Interleukin-6. The first region (<5 Hz) represents the Warburg impedance of our equivalent circuit. This component, which is created by the diffusion of ions from PBS buffers at low frequencies.

The second region (5 Hz – 1 kHz) represents the capacitance of the electric double layer (EDL). As Interluekin-6 dose concentration increases, the formation of the interleukin-6 antibody complex within the EDL increases the capacitive reactance and causes the observed shift in the Nyquist plot in figure 5. As a result, sensing is accomplished through changes in capacitive reactance of the system so that a dose dependent shift in phase may not be apparent. The results indicate that the enhanced surface area resulting from micro-structuring of the micropyramids boosts impedance. Additionally, the highly localized electromagnetic field impacts the impedance of the antibody-antigen-based biosensor. Increasing impedance through resonance represents a novel and relatively unexplored approach in impedance analysis, as it facilitates the detection of surface property changes owing to the highly concentrated electrons near the surface. Furthermore, this phenomenon merits further exploration.

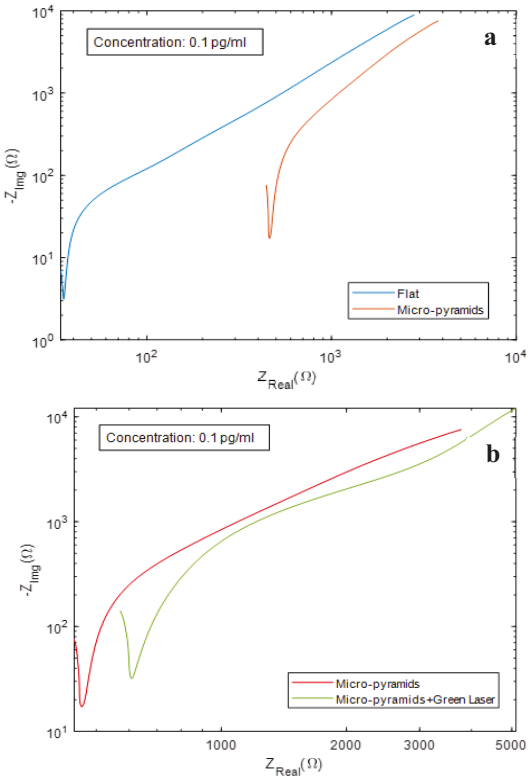

Figure 7. Nyquist plot (a) flat and micropyramids and (b) micropyramids and micropyramids enhanced with green laser (532 nm) at 0.1 pg/ml Int-6 concentration

4. Conclusions

In this study, a sophisticated biosensor platform was meticulously constructed using a two-photon lithographic method, featuring micropyramids on gold electrodes. The process involved careful substrate cleaning, surface activation, precise polymerization, and gold coating, resulting in a highly functional biosensor. The biosensor was further prepared for effective biomolecule immobilization, involving the binding of interleukin-6 (Int-6) antibodies to the micropyramids using a cross-linker. This preparation was critical for the biosensor's biosensing capabilities. Experimental results demonstrated that the presence of micropyramids significantly enhanced the biosensor's performance, allowing for the detection of varying concentrations of Int-6. The increased surface area provided by the micropyramids contributed to improved sensitivity. Additionally, the introduction of a green laser (532nm) further enhanced the biosensor's performance, increasing impedance measurements compared to the absence of laser illumination. In conclusion, this biosensor platform, with its micro-pyramid structures and laser enhancement, shows promise for advanced biosensing applications. It offers increased sensitivity and specificity for the detection of biomolecules like interleukin-6. Further research and development in this direction hold potential for valuable applications in healthcare and beyond.

Acknowledgements

This material is based upon work supported in part by the National Science Foundation under Grant number 2050887 and 2018853. The opinions, findings, and conclusions, or recommendations expressed are those of the author(s) and do not necessarily reflect the views of the National Science Foundation. The team extends its gratitude to the Office of Undergraduate Research for Student Internal Grant their generous support in funding the research experience for the student.

References

[1] B. Heidt, W.F. Siqueira, K. Eersels, H. Diliën, B. van Grinsven, R.T. Fujiwara, T.J. Cleij, Point of Care Diagnostics in Resource-Limited Settings: A Review of the Present and Future of PoC in Its Most Needed Environment, Biosensors (Basel) 10(10) (2020).

[2] G.J. Kost, N.K. Tran, Point-of-Care Testing and Cardiac Biomarkers: The Standard of Care and Vision for Chest Pain Centers, Cardiol Clin 23(4) (2005) 467-90, vi.

[3] B. Jagannath, K.C. Lin, M. Pali, D. Sankhala, S. Muthukumar, S. Prasad, Temporal profiling of cytokines in passively expressed sweat for detection of infection using wearable device, Bioeng Transl Med 6(3) (2021) e10220.

[4] J. Li, F. Madiyar, S. Ghate, K.S. Kumar, J. Thomas, Plasmonic organic electrochemical transistors for enhanced sensing, Nano Research 16(2) (2023) 3201-3206.

[5] P.K. Vabbina, A. Kaushik, N. Pokhrel, S. Bhansali, N. Pala, Electrochemical cortisol immunosensors based on sonochemically synthesized zinc oxide 1D nanorods and 2D nanoflakes, Biosensors and Bioelectronics 63 (2015) 124-130.

[6] M. Frasconi, M. Mazzarino, F. Botrè, F. Mazzei, Surface plasmon resonance immunosensor for cortisol and cortisone determination, Analytical and Bioanalytical Chemistry 394(8) (2009) 2151-2159.

[7] D. Kinnamon, R. Ghanta, K.-C. Lin, S. Muthukumar, S. Prasad, Portable biosensor for monitoring cortisol in low-volume perspired human sweat, Scientific Reports 7(1) (2017) 13312.

[8] T. Hirano, S. Akira, T. Taga, T. Kishimoto, Biological and clinical aspects of interleukin 6, Immunol Today 11(12) (1990) 443-9.
[9] A. Benedetto, P. Ballone, Room temperature ionic liquids interacting with bio-molecules: an overview of experimental and computational studies, Philosophical Magazine 96(7-9) (2016) 870-894.
[10] F. Sjögren, C. Anderson, Sterile trauma to normal human dermis invariably induces IL1beta, IL6 and IL8 in an innate response to "danger", Acta Derm Venereol 89(5) (2009) 459-65.
[11] R.S. Jawa, S. Anillo, K. Huntoon, H. Baumann, M. Kulaylat, Analytic review: Interleukin-6 in surgery, trauma, and critical care: part I: basic science, J Intensive Care Med 26(1) (2011) 3-12.
[12] V.J. Ellison, T.J. Mocatta, C.C. Winterbourn, B.A. Darlow, J.J. Volpe, T.E. Inder, The relationship of CSF and plasma cytokine levels to cerebral white matter injury in the premature newborn, Pediatr Res 57(2) (2005) 282-6.
[13] M. Helle, L. Boeije, E. de Groot, A. de Vos, L. Aarden, Sensitive ELISA for interleukin-6. Detection of IL-6 in biological fluids: synovial fluids and sera, J Immunol Methods 138(1) (1991) 47-56.
[14] S. Tanguay, J.J. Killion, Direct comparison of ELISPOT and ELISA-based assays for detection of individual cytokine-secreting cells, Lymphokine Cytokine Res 13(4) (1994) 259-63.
[15] L.S. Ardekani, P.W. Thulstrup, Gold Nanoparticle-Mediated Lateral Flow Assays for Detection of Host Antibodies and COVID-19 Proteins, Nanomaterials (Basel) 12(9) (2022).
[16] G. Liu, C. Jiang, X. Lin, Y. Yang, Point-of-care detection of cytokines in cytokine storm management and beyond: Significance and challenges, View (Beijing) 2(4) (2021) 20210003.
[17] U. Turpeinen, E. Hämäläinen, Determination of cortisol in serum, saliva and urine, Best Practice & Research Clinical Endocrinology & Metabolism 27(6) (2013) 795-801.
[18] Y. Li, L. Liu, L. Qiao, F. Deng, Universal CRISPR/Cas12a-associated aptasensor suitable for rapid detection of small proteins with a plate reader, Front Bioeng Biotechnol 11 (2023) 1201175.
[19] J. Plou, P.S. Valera, I. García, C.D.L. de Albuquerque, A. Carracedo, L.M. Liz-Marzán, Prospects of Surface-Enhanced Raman Spectroscopy for Biomarker Monitoring toward Precision Medicine, ACS Photonics 9(2) (2022) 333-350.
[20] N. Dutta, P.B. Lillehoj, P. Estrela, G. Dutta, Electrochemical Biosensors for Cytokine Profiling: Recent Advancements and Possibilities in the Near Future, Biosensors (Basel) 11(3) (2021).
[21] A.-I. Bunea, N. del Castillo Iniesta, A. Droumpali, A.E. Wetzel, E. Engay, R. Taboryski, Micro 3D Printing by Two-Photon Polymerization: Configurations and Parameters for the Nanoscribe System, Micro 1(2) (2021) 164-180.
[22] Z. Faraji Rad, P.D. Prewett, G.J. Davies, High-resolution two-photon polymerization: the most versatile technique for the fabrication of microneedle arrays, Microsystems & Nanoengineering 7(1) (2021) 71.
[23] R. Srinivasaraghavan Govindarajan, T. Stark, S. Sikulskyi, F. Madiyar, D. Kim, Piezoelectric strain sensor through reverse replication based on two-photon polymerization, SPIE2022.
[24] R.D. Munje, S. Muthukumar, A. Panneer Selvam, S. Prasad, Flexible nanoporous tunable electrical double layer biosensors for sweat diagnostics, Scientific Reports 5(1) (2015) 14586.
[25] E.P. Randviir, C.E. Banks, Electrochemical impedance spectroscopy: an overview of bioanalytical applications, Analytical methods 5(5) (2013) 1098-1115.

BIOGRAPHY

Foram Madiyar, *is Assistant Professor, Program Coordinator for Chemistry, and Directors of Nanomaterials Lab at Embry Riddle Aeronautical University, Daytona Beach, FL. She has received B.S. Pharmaceutical Sciences from Pune University India and Ph.D. in Chemistry from Kansas State University. Her research focuses on polymers, self-healing materials, smart materials, nanotechnology, which deals with matter, materials, and devices at the nanoscale. She has a passion of involving and empowering undergraduate students in the undergraduate research programs and experiences by exposing them to interdisciplinary sciences such as organic chemistry, Engineering Physics, aerospace engineering microfabrication, synthetic chemistry, molecular biology, surface chemistry, and medicine. Current and future prospects of research will be focused on the development of products and technology solutions in the fields of Aerospace and Healthcare applications using various aspects of nanoscience.*

Sahil Ghate is Masters student in Unmanned Aircraft systems, and completed his bachelors in Aerospace engineering from Embry Riddle Aeronautical University. He involved in leading edge research in rotor blade aerodynamics, nano-materials, smart materials, and electro-chemical sensor with plasmonic and micromaterials for the biosensor applications in health care with extensive experience in computer-aided design (CAD), system modeling, prototyping, and electrical instruments.

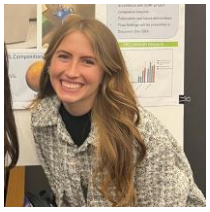

***Kaitlyn Nielsen**, Undergraduate student perusing bachelors in Aerospace Physiology, at Embry Riddle Aeronautical University. Her interests lies in investigating the extreme environmental effects on microbial, plant and human health.*

***Rishikesh Srinivasaraghavan Govindarajan** is a final-year PhD researcher in Aerospace Engineering, specializing in Structural and Composite materials. He holds a Master's degree in Aerospace Engineering from Embry Riddle Aeronautical University. His expertise includes Structural Health Monitoring and Non-Destructive Testing (NDT) applications, with a focus on developing cost-effective smart sensing systems using Additive Manufacturing. His research involves a wide range of experimental techniques, including SEM, EDX, FTIR, Raman, XRD, DIC, DSC, DMA, CT-Scan, PVD, and Nanointender analysis. Additionally, he is proficient in engineering software such as CATIA, FEMAP, SolidWorks, ANSYS, and COMSOL Multiphysics.*

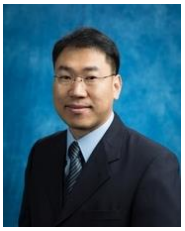

Dr. Daewon Kim is a Professor of Aerospace Engineering and the Director of SMART Lab at Embry-Riddle Aeronautical University's Daytona Beach campus. He holds both bachelor's and master's degrees from Embry-Riddle and a doctoral degree from Virginia Tech. He is interested in additive manufacturing, smart materials, structural health monitoring, soft actuators and sensors, adaptive structures, and space structural systems. He is currently working on several research projects including embedded sensors, micro/macro additive manufacturing, rapid adaptive structures, soft robotics, space origami structures, and space debris removal projects.